

Applications of Spectroscopic Techniques for Polymer Nanocomposite Characterization

MARYAM BATOOL (✉ maryambatool6666@gmail.com)

UNIVERSITY OF SAHIWAL, SAHIWAL <https://orcid.org/0000-0003-2165-6562>

Muhammad Nouman Haider

Government College University Faisalabad

Tariq Javed

University of Sahiwal

Research Article

Keywords: Spectroscopy, Polymer, Nanocomposites, Characterization, Fluorescence, solid-state nuclear magnetic resonance, infrared spectroscopy, Raman spectroscopy

Posted Date: December 8th, 2021

DOI: <https://doi.org/10.21203/rs.3.rs-1039893/v2>

License: © ⓘ This work is licensed under a Creative Commons Attribution 4.0 International License.

[Read Full License](#)

1 Applications of spectroscopic techniques for polymer 2 nanocomposite characterization

3 *Maryam Batool* ^{1(a)*}, *Muhammad Nouman Haider* ^{2(a)} and *Tariq Javed* ^{1(b)}

4 *Department of Chemistry, Government College University Faisalabad, 38000, Punjab,*
5 *Pakistan* ^{2(a)}

6 *Department of Chemistry, University of Sahiwal, 57000 Sahiwal, Punjab, Pakistan*
7 ^(1a*, 1b)

8 nomanh923@gmail.com ^{2(a)} maryambatool6666@gmail.com or

9 <https://orcid.org/0000-0003-2165-6562> ^{1(a)*} and mtariq@uosahiwal.edu.pk ^(1b)

10 * Corresponding author: *Maryam Batool*

11 Email: maryambatool6666@gmail.com

12 Contact number: 0300-0080022

13 ABSTRACT

14 During past decades, spectroscopic techniques find wide range of applications ranging from
15 biological applications to the measurement of chemical composition and characterization of
16 variety of substances i.e., polymers, nanocomposites etc. Nanocomposites are emerging and
17 growing materials having wide variety of uses. To study the characteristic properties,
18 characterize, and development of new materials using polymer nanocomposites, several
19 molecular characterization techniques are available and are in use today. Principle objective
20 of this review is to summarize the knowledge in current characterization techniques and to
21 study the applications of fluorescence, solid-state nuclear magnetic resonance (NMR),
22 infrared, besides Raman molecular characterization techniques for characterization of
23 polymers, filler, and composites. Fluorescence technique did not provide detailed analysis of
24 materials while solid-state NMR spectroscopy determine silanol hydroxyl groups at the silica
25 exterior in addition to their interactions with polymer and polymer-filler interfacial interactions
26 (via relaxation time). For characterization of various kinds of functional groups in polymer/
27 fillers, infrared spectroscopy employed. While Raman spectroscopy finds extensive
28 applications for analysis of carbon-based materials. Novelty of this review is that till yet very
29 few review papers have been published which briefly describe all these mentioned techniques
30 along their applications in a very simple and an effective way.

31 Keywords: Spectroscopy, Polymer, Nanocomposites, Characterization, Fluorescence, solid-
32 state nuclear magnetic resonance, infrared spectroscopy, Raman spectroscopy.

33 Vocabulary

34 Fluorescence: Characterization technique widely used for analysis of exfoliation or intercalation in clay composites.

35 Nanocomposites: Polymer matrix composites having fillers with at least one dimension less than 100 nm are known as
36 polymer nanocomposites which have properties better than traditional composites.

37 Solid-state NMR spectroscopy: Analysis tool for characterization of molecular structure, conformation, and dynamics of
38 polymer chains in various kinds of polymer composites.

39 Infrared spectroscopy: this analysis technique widely used for material characterization via bands/ peaks specific for each
40 functional group of the polymer.

41 Raman spectroscopy: This technique finds extensive applications for characterization of carbon-based materials via
42 resonance-enhanced scattering effects.

43 Introduction

44 Nanomaterials i.e., spheres, sheets, as well as rods etc. spread in polymer materials found numerous applications and
45 study in rubber nanocomposites owing to their improved mechanical, electrical besides thermal characteristics. When
46 these filler elements are spread inside polymer matrix, it resulted in the extraordinary interfacial area amongst organic
47 and inorganic phases and interfacial connections amongst these two phases (governs the level of matrix strengthening)
48 [1]; [2].

49 Importance of interfacial adhesion besides filler dispersion can be determined through stationary in addition to active
50 mechanical performance. Traditional composites (such as those composites in which silica and carbon black are used as
51 fillers) show upsurge in elastic modulus besides tensile power owing to strong interface whereas feeble interface resulted
52 in intensification of early composite modulus besides insignificant rise in stress. Silica filled hydrocarbon rubber has
53 weak interface which can be improved by using chemical combining vehicle in the packed structure which is responsible
54 for increasing adhesion amongst filler and rubber [3]. Using sol-gel process (hydrolysis in addition to condensation of
55 inorganic alkoxides of metals such as Si, Ti, Al, Zr, Hf, Ta, Sn etc.) nanosized inorganic structures are produced in situ
56 in rubbers, thermoplastics, and thermosets [4]-[5], [6], [7], [8], [9] which resulted in more fine dispersion of mineral phase with
57 composite development possessing outstanding mechanical, thermal and optical characteristics.

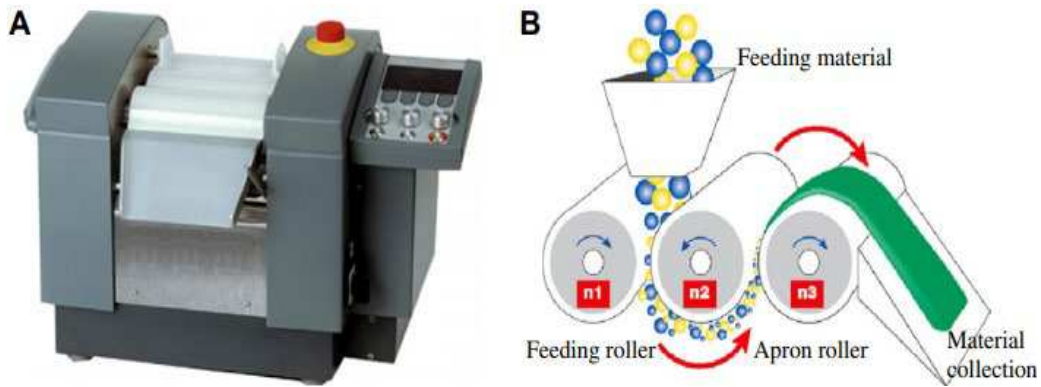
58 To achieve great interfacial region designed for polymer-filler interaction, high level of distribution as well as small
59 sized particles are involved. In poly (dimethyl siloxane) (PDMS) networks, together with silica particles as fillers,
60 polymer-filler interactions are attained by means of hydrogen bonding amongst hydroxyl parts of silica exterior as well
61 as oxygen atoms of polymer chains [10]-[11]. Higher modulus and higher extensibility can be achieved when Silica-titania
62 mixed-oxide fillers are used in PDMS networks as compared with those networks where single filler are used [12]-[13].

63 Research on composites centered over layered silicates comprised of stacked parts of one to a several nm wide started
64 following manufacturing of nylon 6/ clay nanocomposites by the Toyota Research Group. The purpose behind this is to
65 attain exfoliated structure in which silicate sheets remain evenly spread in host medium [14]- [15], [16], [17]. Exfoliated
66 nanocomposites have the benefit of being utilized in food packing owing to their reduced penetrability to gas and water
67 vapors [18]. In situ polymerization procedure or traditional melt working ways i.e., extrusion or injection molding are
68 useful for preparation of clay nanocomposites. Poor electrical conductivity of clay nanocomposites can be overwhelmed
69 by the addition of conductive insertions (such as small number of carbon-based materials). Physical performance of
70 composite can be improved through two fold filling method such as using spheres besides rods [19], or spheres in addition
71 to plates [20].

72 As compared to traditional carbon black, carbon nanomaterials, such as carbon nanotubes, graphite or graphene possess
73 excellent electrical conductivity, mechanical power combined with high aspect ratios. Owing to these characteristics, they
74 are known as advanced reinforcing fillers for polymeric matrices. Exceptional structure (made up of cylinders of single
75 or additional graphene layers) of carbon nanotubes (CNTs) make it more useful carbon nanostructure [2]. A lot of work
76 has been performed on methods used for dispersal of CNTs within polymer matrix. Among them calendaring is widely
77 used way, its principle and calendaring mechanism is shown in

78 Fig. 1. However, various findings showed poor spreading or dispersal of CNTs within polymer matrix (owing to lack of
79 interfacial adhesion in addition to their capacity to pack together. In order to achieve their good dispersion and contact
80 with polymer chains functionalization of tube exterior is carried out [21].

81



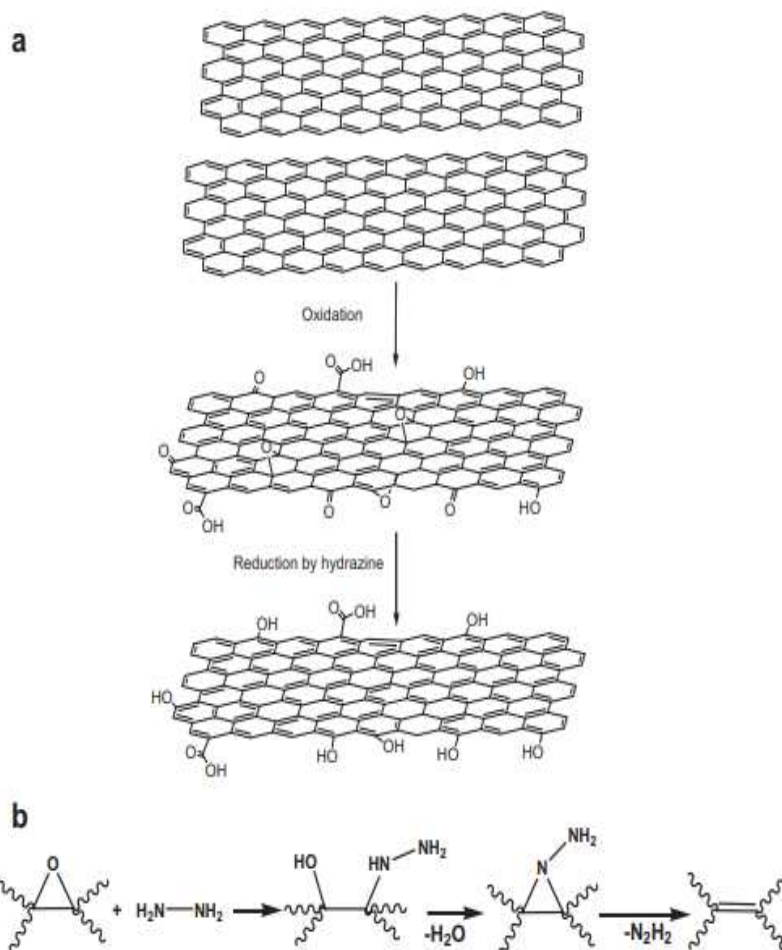
83
84 Fig. 1| (A) Calendaring machine for particle spreading into polymer medium (B) Working mechanism of calendaring
85 process (image reprinted with permission) [21].

86
87 Punetha et al. debated numerous approaches and practices with their applications for carbon nanomaterials
88 functionalization [22]. Zhang et al. discovered that photochromic molecules, such as use of azobenzenes, diarylethenes,
89 spiropyrans/ oxazines and stilbenes for carbon nanomaterials functionalization is accountable for their additional
90 characteristics [23].

91 Several techniques have been established intended for attaining sole sheets by means of graphite intercalation
92 compounds. Masses of graphene known as graphite nanostructures or graphite nanoplatelets (GNPs) with 1-10 nm
93 thickness are the result of these techniques. However, Raman spectroscopy showed several structural flaws when
94 chemical alteration of graphite yield graphene. Oxidation of graphite towards graphene oxide after which it reduced to
95 form graphene (a), and mechanism of reduction by hydrazine (b), is shown in

96 Fig. 2 [24].^{[25], [26], [27]}. Owing to low conductivity, resultant oxidized material is not used as conductive filler. Additional
97 information regarding the production, processing requirements of various graphite nanostructure, and their (graphite-
98 graphene grounded nanocomposites) characterization can be found in literature [28].^{[29], [30], [31], [32], [33], [34], [35]}.

99 Above debate revealed that a complete understanding of the composite and its properties is required before their use
100 and, in this regard, molecular spectroscopy is supportive which offers molecular level characterization. This review article
101 focuses on uses of molecular spectroscopy such as fluorescence, solid-state NMR, infrared, as well as Raman
102 spectroscopy etc. aimed at polymer composite investigation besides quoting examples of the grouping of atomic force
103 microscopy and infrared spectroscopy (AFM-IR) and tip-enhanced Raman scattering (TERS) for the purpose to achieve
104 chemical information with nanometric spatial resolution.
105



107
108
109
110

Fig. 2| (a) Graphite oxidation to graphene oxide which is then reduced to form graphene, (b) mechanism of reduction by hydrazine (image reprinted with permission) [24].

Box 1| unique properties of polymer nanocomposites

polymer matrix composites having fillers with at least one dimension less than 100 nm are known as polymer nanocomposites. These polymer nanocomposites are of great interest in modern's world owing to several reasons which include:

- These polymer nanocomposites have extraordinary large interfacial area because of their small size as compared to that of traditional composites [36]. Additionally, nanoscale fillers possess characteristics different from that of bulk properties of the same raw material e.g., on reducing size of silicon nanoparticles band gap fluctuate which then particle's color [37].
- Since 100 years, elastomeric composites with nanoscale spherical fillers are employed [38]. In the past 15 years, numerous new fillers with multi-functional nanocomposites have been developed. Such as for resistance against scratch, transparent coatings in cell phones and compact-disc technology nanoparticle filled amorphous polymers are extensively employed [39].
- To enhance out-of-plane characteristics and to add conductivity and sensing capabilities of traditional composites nanocomposites are used [40]. Micrometer-scale fillers can cause early disaster in material [41], [42] while on the other hand, nanofillers possess reduced magnitude and provide ductility and toughness to nanocomposites which lessen disaster in composite materials [43], [44], cause upsurge in electrical breakdown strength besides impart durability to these composite materials [45].
- Nanoplatelets, nanoparticles, nanotubes (a) and large volume of interfacial polymer (b) is given below [36]

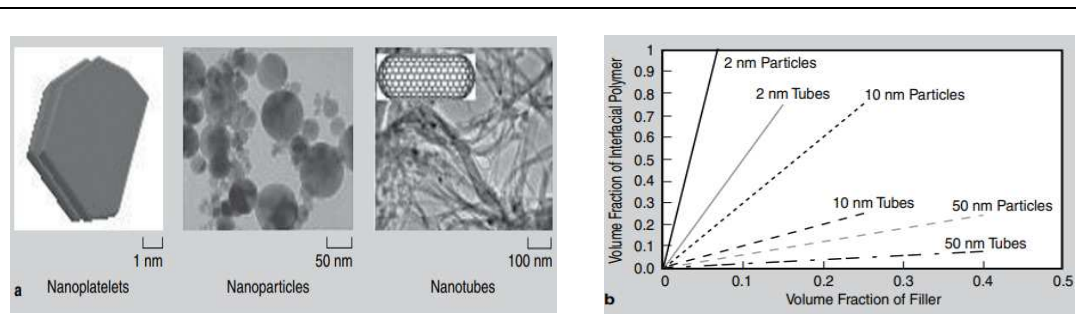


Fig. (a) nanoplatelets (one dimension), nanoparticles (having dimension less than 100 nm), and nanotubes (two dimensions), (b) plot of volume of interfacial polymer centered on interfacial region with thickness of 10 nm surrounding individual nanoparticle and this interfacial region volume has inverse relation with size of nanoparticle (image reprinted with permission) [36].

111

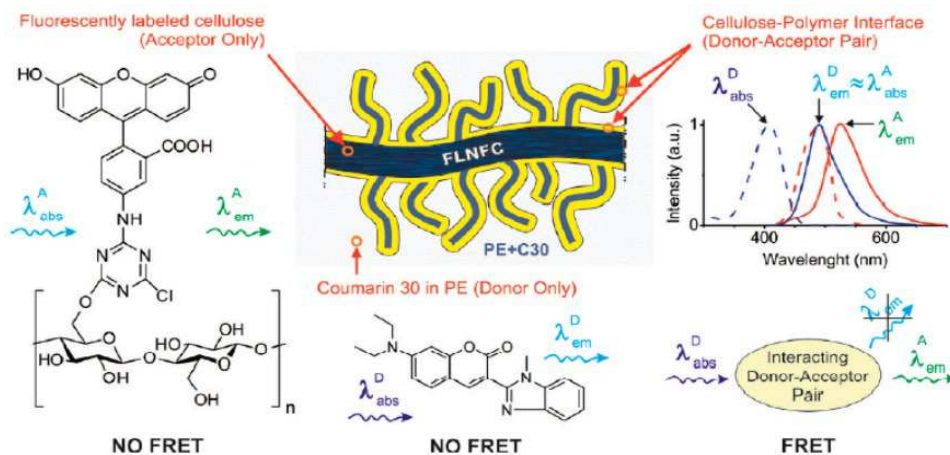
112 Fluorescence Spectroscopy

113

114 In fluorescence spectroscopy, incorporation is achieved in the form of a fluorescent probe employed at a minimal
 115 concentration. Probe incorporated into the polymer matrix yield supporting evidence associated with polymer science
 116 such as changing aspects of polymer chains via excimer fluorescence [46], phase partition in addition to polymer
 117 miscibility, transport methods or polymer deterioration [47].

118 Zammarano et al. employed Förster resonance energy transfer (FRET) for the purpose to investigate interface and
 119 dispersal in polymer nanocomposites. Energy transfer amongst donor (fluorophore in an excited electronic state) to an
 120 acceptor one is best defined by FRET mechanism. This energy transfer takes place via nonradiative dipole-dipole
 121 coupling. FRET process is highly dependent on distance that is 1 to 10 nm between two molecules. This process is used
 122 to study the nanofeatures at border of a polymer–filler system. They studied dispersal of the supporting phase with
 123 nanofibrillated cellulose (NFC) fluorescently labelled with 5-(4,6-dichlorotriazinyl) aminofluorescein (FL), acting as
 124 acceptor, which is distributed on polyethylene doped with Coumarin 30 (C30), acting as a donor. Use of FRET for
 125 interface study in polymer composite is given in

126 Fig. 3 [48].



128

129 Fig. 3| Graphic representation of use of FRET to study/ reveal interface in polymer composites (image reprinted with
 130 permission) [48].

131

132 For melt-process polymer clay nanocomposite analysis of intercalation and exfoliation, fluorescence, behavior of
 133 optical probes (Nile Blue A besides methylene blue) in polystyrene in addition to polyamide-6 play a vital role [49].
 134 Results of incarceration on glass transition temperature along with physical aging in polystyrene, poly (methyl
 135 methacrylate) and poly (2-vinyl pyridine) nanocomposites was studied using fluorescence having 10 to 15 nm diameter
 136 silica nanospheres or 47 nm diameter alumina nanospheres [50].

137 Fluorescence spectroscopy is also helpful in studying stress-softening process in filled elastomers (since filled
 138 elastomers have high tensile strength) and this process is known as Mullin's effect. Clough et al. worked on the stress-
 139 softening effect and observed that mechano-luminescence on bis (adamantyl)-1,2 dioxetane (mechanophore) hold inside
 140 the cross-linker and 9,10-diphenylanthracene (DPA) were contained in silica-filled poly (dimethyl siloxane) break down

141 mechanophore and forms ketone in excited state which then come to ground state and eliminate light which was taken up
 142 by DPA (acting as an acceptor molecule) in this case. Process of this energy transfer is FRET mechanism involving donor
 143 and acceptor molecules for energy transfer [51].

144

145 **Solid-state NMR spectroscopy**

146

147 Sensitivity of NMR spectra along with relaxation factors to the polymer chains are the basis which form solid-state NMR
 148 spectra as suitable spectra for study of polymer-filler interfaces. To distinguish polymer performance in interfacial section
 149 from bulk, solid-state NMR spectra was applied. Formulae (transverse magnetization relaxation function) used to find
 150 out two dissimilar spin-spin relaxation times, T₂, linked to polymer in solid-state proton NMR studies is given below:

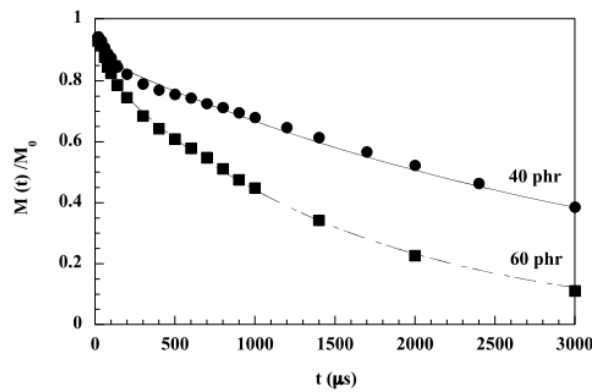
151
$$M(t) = M_0 \exp\left[-\frac{t}{T_2^{mob}}\right] + (1 - M_0) \exp\left[-\frac{t}{T_2^{rig}}\right]$$

152 Where; T₂^{mob} is spin-spin relaxation time linked to polymer in the bulk while T₂^{rig} is spin-spin relaxation time of
 153 polymer present at interface and M₀ is portion of mobile chains external to adsorption coating. Formulae employed to
 154 find width of interfacial layer is given below:

155
$$e = R \left[\left(1 + \frac{\omega(1-\phi)}{\phi}\right)^{\frac{1}{3}} - 1 \right]$$

156 Where: ω is portion of polymer, which is immobilized, φ is volume portion of filler while R is radius of particles
 157 studied. Dewimille et al. observed thickness of 1.5 nm in his work. In case of tin-catalyzed silica-filled poly (dimethyl
 158 siloxane) composites, proton NMR relaxation statistics is given in Fig. 4 [10].

159



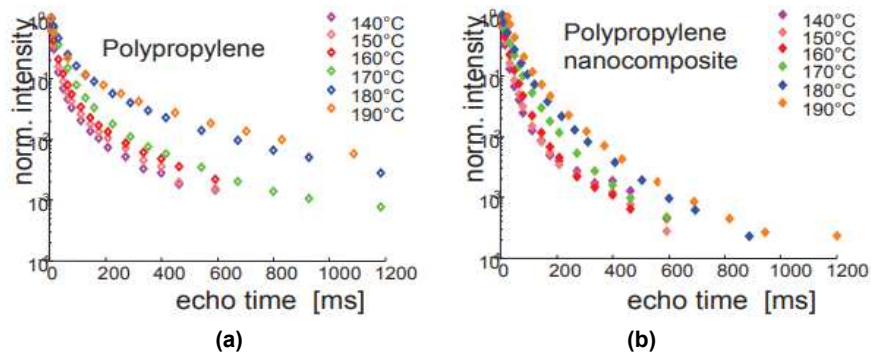
161 Fig. 4| Tin-catalyzed silica-filled poly (dimethyl siloxane) composites, proton NMR relaxation statistics (image
 162 reprinted with permission) [10].

163

164 Böhme and Scheler worked on poly (propylene) as well as a poly (propylene nanocomposite) and investigated
 165 temperature measurement in melt. Results showed (given in

166 Fig. 5) that in both samples (pure and nanocomposite polymer), relaxation period shows the probable two component
 167 decay. From results, it was found that in case of pure polymer, longer component has direct relationship with temperature
 168 and motion of polymer chains has direct relation with temperature. While in case of nanocomposite, temperature has less
 169 influence on chains mobility as compared to unadulterated polymer. The cause of this constrained motion is the interaction
 170 of filler with polymer chains leading to restricted motion of polymer chains [52].

171



173

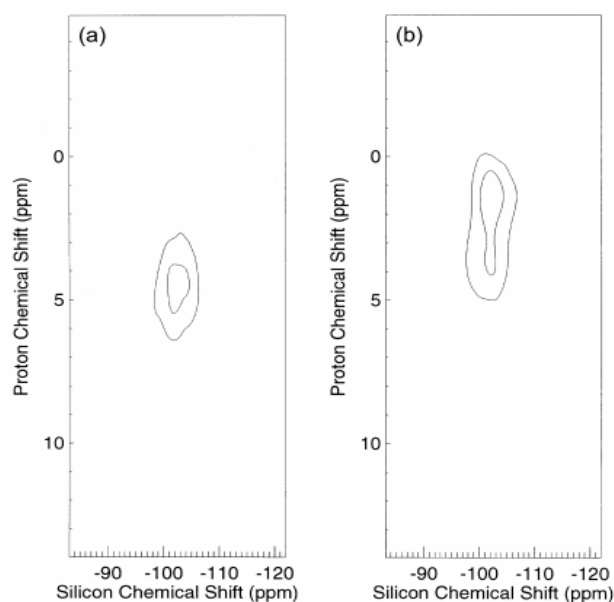
174

175 Fig. 5| Results of T2 statistics for poly (propylene) (a) and Poly (propylene) nanocomposite (b) as a function of
176 temperature (image reprinted with permission) [52].

177

178 Solid state NMR finds applications in characterization of polymers, chemical shift extent, line forms in addition to
179 relaxation time [53]. [54]. Proton–proton double quantum correlation spectroscopy, heteronuclear correlation NMR or
180 solid-state deuterium quadrupolar-echo spectra also used in addition to solid state NMR spectra for the investigation of
181 polymer interface properties [18].

182 To study poly (ethyl acrylate)/ vycor composite having a 50-microsecond as well as a 50-millisecond spin diffusion
183 delay time, the interface, proton–silicon heteronuclear correlation trials were used. For spin diffusion, 50-microsecond is
184 short and a correlation amongst proton at 4.5 ppm and Q_3 vycor silicon surface sites was observed which is given in Fig.
185 6 (part a) while Fig. 6 (part b) represent connection amongst polymer protons at 1.3 ppm and 4 ppm besides Q_3 vycor
186 silicon surface sites having spin dispersal delay of 50 millisecond. From this observation, authors make conclusion that
187 central space of the pore is engaged by the polymer and water layer provides insulation to it from silica surface [55].
188



190 Fig. 6| 2D proton–silicon heteronuclear correlation spectra for the poly (ethyl acrylate)/ vycor composite having (a)
191 50-microsecond in addition (b)50-millisecond spin diffusion delay time (image reprinted with permission) [55].

192 For analysis of poly (methyl methacrylate) (PMMA)-based hybrids with modified silica ($mSiO_2$) nanoparticles [56].
193 Characterization and measurement of relaxation time of SiO_2 and $mSiO_2$ by Si solid-state NMR indicate longer values
194 in the relaxation time of the $mSiO_2 - g - PMMA$ phase in comparison to clear polymer. Additionally, there is an upsurge
195 in the values of T_g of 6 and 12 °C in both nanocomposite of PMMA with neat silica and with modified silica ($mSiO_2$)
196 respectively as compared to PMMA. For the purpose to examine the phase structures along with phase dynamics in both
197 exfoliated and intercalated nanocomposites, variations in molecular motion and relation between two components, solid-
198 state NMR spectroscopic analysis of polymer/ clay nanocomposites was carried out [57], [58].

199 Infrared and Raman Spectroscopy

200 Vibrational properties of polymers help to determine the information about polymeric systems using molecular
201 spectroscopies such as Infrared and Raman spectroscopy. When frequency of incident infrared radiations resonates with
202 the specific vibrational mode, then from this kind of resonance interaction infrared radiation spectra occurs (used for thin
203 film study of polymers) and inelastic scattering of light, when a light from a monochromatic source is given to a molecule,
204 resulted in the Raman effect (for investigation of thick films of polymers) [18].

205 **Infrared spectroscopy.** Cole studied applicability of the infrared spectroscopy intended for characterization purposes i.e.,
206 characterizing state of intercalation as well as exfoliation in polymer nanocomposites made from montmorillonite-
207 founded nano clays. Results showed that form of clay Si-O band envelope amongst 1350 as well as 750 cm^{-1} as a function
208 of processing (which is because of good intercalation and exfoliation). Author also claimed that these results are also due
209 to the fact that when some kind of compatibilizing agent was added to the clay it resulted in the formation of connections
210 amongst this capitalizing agent as well as Si-O dipoles of nano clay [59].

211 To characterize state of dispersal of layered silicate in polymer nanocomposite grounded on poly (hexamethylene
 212 isophthalamide) (aPA) as well as montmorillonite nanoclay (MMT), Zhang et al. employed Fourier transfer infrared

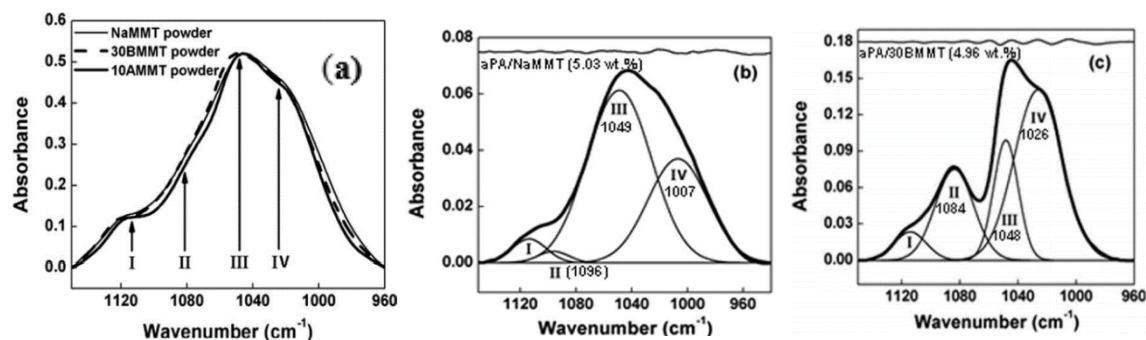


Fig. 7] FTIR spectra of sodium montmorillonite (NaMMT), 30 BMMT, and 10 AMMT powder. Peaks I, II, III, and IV are positioned at 1100, 1082, 1050, and 1030 cm^{-1} correspondingly. (b) FTIR difference spectra of Si-O stretching region for aPA nanocomposites having NaMMT with 5 % clay loading. Maximum peak occurs at 1096, 1049, and 1006.9 cm^{-1} . (c) FTIR difference spectra of Si-O stretching region for aPA nanocomposites having 30BMMT with 5 % clay filling. Maximum peak occurs at 1083.7, 1048, and 1026 cm^{-1} . Position of peaks (i.e., peak II, III and IV) is labelled and curves in each spectrum best describe the difference between actual data and the best fit curve. (Image reproduced with permission).

213 (FTIR) spectroscopy. The Si-O band envelope of NaMMT (sodium montmorillonite), as well as two organoclays (given
 214 in **Error! Reference source not found.** a) shows four usual components. It was also noted that infrared spectra of these
 215 both clays and pristine clays are almost like each other which makes it clear that absorption band of agglomerated
 216 nanoclay powder does not affect by intercalated organic surfactants. In polymers with unmodified clay particles, the
 217 obtained spectral pattern is wider with lesser intensity (shown in **Error! Reference source not found.** b) as compared
 218 with delaminated organoclay in same matrix (given in **Error! Reference source not found.** c). Out of plane vibration
 219 mode of Si-O bond (shown by peak II) shifts towards lower wavenumbers while in plane vibration mode of Si-O bond
 220 (shown by peak IV) shifts toward higher wavenumbers in exfoliated structure. As of this study, it can be concluded that
 221 clay dispersal in host polymeric matrix can be indicated with the help of clay Si-O band envelope [60].

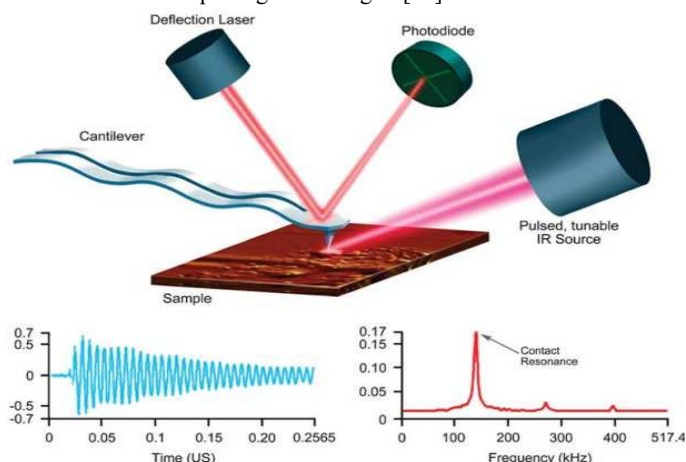
222 Infrared spectroscopy reveals that the surface alteration of carbon nanotubes throughout functionalization procedure
 223 has remarkable effect in improving compatibility of carbon material together with polymer matrix [61], [62], [63]. Lee et
 224 al. worked on surface modification of carbon nanotube composites using acid, heat, and hydrogen peroxide. First, acid
 225 treatment (a two-step mechanism) was carried out. For this purpose, 65 % solution of 3:1 mixture of H_2SO_4/HNO_3
 226 in water was used followed by ultrasonic excitation to the suspension for 1 hour keeping the temperature 80 °C. This acid
 227 treatment resulted in attachment of carboxyl as well as hydroxyl groups on the exterior of CNTs. After this, CNTs was
 228 washed by distilled water after which filtration and drying occur in vacuum oven at 50 °C for 2 days. In hydrogen peroxide
 229 treatment, CNTs were distributed in 1:1 mixture of H_2O_2 / distilled water for introducing hydroxyl as well as carboxyl
 230 groups over the exterior of CNTs. After this hydrogen peroxide treatment, washing, filtration and drying of sample was
 231 carried out. In third treatment, i.e., heat treatment, heating was done for one hour in a furnace at 500 °C with air circulation.
 232 Infrared spectrum of H_2O_2 treated CNTs showed strong band at 1089 cm^{-1} which relates to the presence of many C-O
 233 bonds on exterior of the CNTs as a result of hydrogen peroxide treatment (resulting in improved stability of poly (amide/
 234 imide)/ CNT composite towards heat) [64].

235 Deniz et al. worked on poly (vinylpyrrolidone) PVP incorporating with gold nanoparticles and showed from infrared
 236 analysis that there were interactions between carbonyl groups of PVP i.e., poly (vinylpyrrolidone) and metal particles
 237 [65]. Al-Attabi et al. worked on preparation as well as characterization of polyurethane composites comprising graphene
 238 along with gold nanoparticles. FTIR results revealed that there are no strong connections amongst the polymer chains
 239 plus merged fragments. Moreover, mechanical properties and tensile strength of modified polyurethane (AuNPs/
 240 graphene/ PU composites) are poor as compared to unmodified polyurethane. This is because of the reason that particle
 241 agglomeration creates a lot of imperfections within the composite matrix leading to poor mechanical strength [66].

242 When Ag nanoparticles were added to Polyaniline/ diamond/ functionalized multi-walled carbon nanotubes
 243 (MWCNTs), then their characterization shows a peak on 1036 cm^{-1} which confirms an interactions amongst polyaniline
 244 plus silver nanoparticles [67]. Infrared spectroscopy also finds applications in analysis of orientations of polymer chains
 245 occurring uniaxially-unfilled as well as filled elastomeric networks. Study of orientation performance of filled networks
 246 leads to the assessment of the degree of bonding amongst polymer and filler [68], [69]. Infrared spectroscopy also useful
 247 in quantification (by determining the quantity of reactive spots for each nm^2 of filler exterior) of degree of bonding of
 248 network layers to filler exterior [70].

249 Cole et al. find out orientation of equally polymer chains as well as clay platelets in blown films of composites founded
250 on polypropylene along with clay particles using infrared spectroscopy and “the tilted film method”. They concluded that
251 clay orientation was relatively high-level owing to high anisometric nature of that kind of filler as compared to those
252 polymer chains having modest level of orientation [71]. However, in work of Bokobza et al. it was found that there was
253 no such great change in extent of molecular orientation of polystyrene (PS) after carbon nanotube addition. The possible
254 reason of this is that orientation of both main chain ($-CH_2-$) segments and side groups (i.e., benzene ring) of the
255 polystyrene macromolecule hampers throughout the extending of nanocomposite films [72].

256 AFM-IR technique, used for the purpose to get infrared spectra with nanoscale spatial resolution, has been reported in
257 detail by Dazzi et al. [73]. Limitations of traditional infrared spectroscopy technique are overcome using AFM-IR
258 technique (combination of atomic force microscopy along with infrared spectroscopy). Applications of this technique
259 include polymers, life sciences, photonics, solar cells etc. Marcott et al. describe some applications of AFM-IR technique
260 in the field of polymer composites. These comprised of an isotactic poly (propylene film) in which SiO_2 particles were
261 added, polymer having carbon black particles as well as a carbon-fiber/ epoxy composite material. Information regarding
262 interphase region amongst specific nanomaterial addition along with bulk polymer can be achieved using AFM-IR
263 technique. An illustration of AFM-IR technique is given in Fig. 8 [74].



265 Fig. 8] AFM-IR technique involves the use of pulsed, tunable IR source (for excitation of molecular resonances in
266 trial). Thermal expansion occurs when IR radiations are absorbed leading to excitation of resonant oscillations of
267 cantilever. Cantilever oscillations decline in characteristic ringdowns (underneath left-hand). Fourier techniques were
268 used to analyze these ringdowns for the purpose to bring out their amplitude as well as frequency (underneath right-
269 hand). Contact resonance peak frequencies of cantilever ringdowns determine mechanical toughness of sample
270 (image reprinted with permission).

271 **Raman spectroscopy.** With the advent of carbon nanotubes in previous two decades, use of Raman spectroscopy for
272 analysis of carbon-based composites revived [75]. This technique widely used for characterization of vibrational states
273 of wide-ranging range of carbon-centered materials like graphene, graphite, diamond, along with carbon nanotubes etc.
274 Raman spectroscopy is one of the best significant practices meant for study of carbon-centered composites for reason that
275 these composites create solid, well defined bands even at their low concentration owing to resonance-enhanced Raman
276 scattering effects [76]. However, some factors such as strain, pressure, filler-filler as well as polymer-filler interactions,
277 orientation, temperature, plus functionalization etc. disturb spectral features of carbon materials [77].

278 Laser-induced sample heating shifts vibrational Raman modes of carbon-based materials and are suggested by Everall
279 et al. for use in order to interpret precise Raman data [78]. Laser heating effects of the sample cause an upsurge in the
280 confined temperature shifting the Raman bands towards lower wavenumbers equally for pristine carbon materials as well
281 as for carbon species implanted in polymeric medium. Shift has direct relation with laser power, however, as detected in
282 numerous cases for carbon materials in polymer matrix shift is lower as matched with non-embedded state [78], [77],
283 [79], [80].

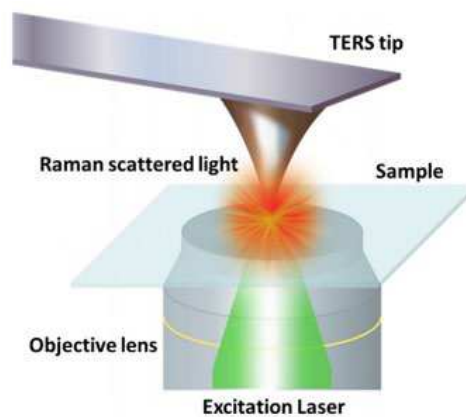
284 By comparing the dispersive behaviour of carbon materials in pure form plus inserted in the matrix, analysis of
285 polymer-filler interface was carried out. Raman spectroscopy has a feature of shifting D as well as G' bands to higher
286 frequencies along with the upsurge in laser excitation energy. For D band, upshift occurs at $50\text{ cm}^{-1}/\text{eV}$ and for G' band
287 its value is $100\text{ cm}^{-1}/\text{eV}$. Electronic properties of carbon materials and the excitation-energy reliance of D as well as G'
288 bands remain greatly concerned by interfacial connections amongst polymer as well as filler. That method has been
289 reviewed previously [76], [81], [82] while Srivastava et al. reported contradicted results in their findings [83].

290 Dispersive behaviour of MWCNTs implanted in polydimethylsiloxane (PDMS) is higher as compared to its pure state.
291 It has also been observed that there exist strong CH- π connections amongst methyl group of PDMS as well as π -electron

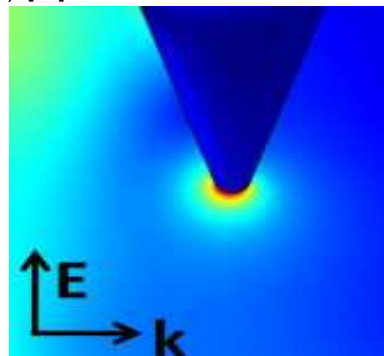
292 rich exterior of carbon nanotube. Modeling studies revealed that a wrapping process around the nanotube exterior takes
293 place owing to extreme elasticity of PDMS chain [84]. CH- π bonding successfully explain the adsorption characteristics
294 of PDMS chains on the CNT exterior which confirms the presence of electrical and mechanical properties in PDMS/
295 CNT composites [85], [84], [86].

296 To overcome the drawbacks of conventional Raman spectroscopy tip-enhanced Raman spectroscopy (TERS) i.e.,
297 grouping of both Raman spectroscopy plus scanning probe microscopy has been used to obtain nanoscale spatial
298 resolution. In this technique, sharpened metal tip is fixated on base of the laser beam as well as can be placed accurately
299 at various areas on sample exterior. Localized surface plasmon (LSP) resonance and antenna effects on tip apex amongst
300 tip-LSPs as well as laser photons improve besides limit electromagnetic (EM) field causing an increase in Raman signal
301 from analyte particles in surrounding area of tip-apex. Further details about advances and technology of TERS can be
302 found in the literature [87], [88]. Schematic diagram of tip-enhanced Raman spectroscopy is shown in Fig. 9 and
303 Fig. 10.

304



306 Fig. 9| Schematic diagram of tip-enhanced Raman spectroscopy showing principle of atomic force
307 microscope (AFM)-centered tip-enhanced Raman spectroscopy (TERS) in transmission manner. Localized surface
308 plasmon (LSP) resonance on tip apex amongst tip-LSPs as well as laser photons improves besides limits
309 electromagnetic (EM) field causing an increase in Raman signal from analyte particles in surrounding area of tip-
310 apex (image reprinted with permission) [87].



312

313 Fig. 10| Incidence of p-polarized laser having electric field (E) parallel to tip-axis on metal resulting in improving EM
314 field intensity to improve besides limits at tip-apex [87].

315

316 Saito and Yanagi worked on β -carotene condensed in single-walled carbon nanotubes (SWCNTs) and analyzed TERS
317 spectra in 100 nm steps all along single tube bundles corresponding to each other. Frequency of encapsulation of β -
318 carotene was not consistent (indicated by lack of β -carotene in certain spectra). This shows the superiority of TERS on
319 the way to prevent averaging of Raman spectra for spatially non-uniform nanocomposite materials [89]. Yano et al.
320 studied nanoscale uniaxial pressure effect on single-walled carbon nanotubes using TERS with tip pressure causing shift
321 in peak position as well as alteration in Raman strength (which indicate tube deformation) [90]. Yano et al. showed that
322 nanoimaging using TERS technique can disclose strain distribution alongside the length of isolated carbon nanotubes
323 [91].

324 Vantasin et al. explained the applications of TERS for study of structure as well as connections of different types of
325 carbon and graphene-centered nanomaterials [92]. Suzuki et al. employed TERS to investigate local connections at
326 boundary of styrene-butadiene rubber (SBR)/ multiwalled carbon nanotube composites (MWCNTs). TERS bands are

327 strong owing to SBR phenyl parts (at strong MWCNT bands) while bands owing to vinyl parts are strong only as soon
328 as MWCNTs are weak. Results indicate that alteration in orientation of phenyl rings with π - π interactions amongst
329 polymer chains as well as MWCNTs is responsible for modification in local distribution of polymer chains [93].

330 Polymer-metal nanocomposites are used in the same way as surface-enhanced Raman scattering (SERS) substrates
331 [94], [95], [96], [97]. SERS is defined as molecular spectroscopic technique which increases Raman intensity of
332 molecules adsorbed on irregular metal exterior specially of silver or gold [98]. Graphene also finds extensive applications
333 in surface-enhanced Raman scattering (SERS). Some aromatic molecules when adsorbed on the exterior of graphene
334 sheet, it causes an upsurge in Raman signal of adsorbed molecules. This upsurge in Raman signal is an indication of
335 strong connections amongst substrate as well as molecules which helps in charge shifting [99]. Metal nanoparticles
336 combined with graphene on the way to build a graphene-mediated surface-enhanced Raman scattering [100].

337

338 Conclusions

339 For the purpose to study the characteristic properties, characterize and development of new materials using polymer
340 nanocomposites, several molecular characterization techniques are available and are in use today. This review article
341 briefly summarizes the knowledge in the current characterization techniques and study the applications of fluorescence,
342 solid-state nuclear magnetic resonance (NMR), infrared, plus Raman molecular characterization techniques for
343 characterization of polymers, filler, and composites. Fluorescence study (for studying/ analysis of exfoliation or
344 intercalation in clay composites), unlike infrared and Raman is not sufficient for detailed analysis of molecular structure.
345 Solid-state NMR is an effective technique (which carry out analysis via determination of relaxation time) for study of
346 region at polymer-filler interface. Infrared spectroscopy, on the other side, is used for material characterization via bands/
347 peaks specific for each functional group of the polymer. Above all, Raman spectroscopy is significant technique meant
348 for chemical analysis of carbon-founded materials which will produce resonance-enhanced scattering effects even at their
349 very small amount in the composite materials.

350

351 Acknowledgements

352

353 First, all praise to Almighty Allah for blessing me with strength and enabling me to successfully accomplish this work. I
354 would like to manifest special thanks my nearest and dearest parents, family, as well as teachers for their endless love,
355 guidance, support, besides encouragement.

356

357 Author's contribution

358 All authors contributed equally to manuscript.

359 Conflicts of interests

360 Authors state no competing financial concerns to influence the work described in this research.

361 REFERENCES

- 362 1. Jancar J, Douglas J, Starr FW, Kumar S, Cassagnau P, Lesser A, et al. Current issues in research on structure–property relationships in
363 polymer nanocomposites. *Polymer*. 2010;51(15):3321-43. doi: <https://doi.org/10.1016/j.polymer.2010.04.074>.
- 364 2. Bokobza L. Mechanical and electrical properties of elastomer nanocomposites based on different carbon nanomaterials. *C—Journal of Carbon*
365 *Research*. 2017;3(2):10. doi: <https://doi.org/10.3390/c3020010>.
- 366 3. Bokobza L. The reinforcement of elastomeric networks by fillers. *Macromolecular Materials and Engineering*. 2004;289(7):607-21. doi:
367 <https://doi.org/10.1002/mame.2004000034>.
- 368 4. Wang S-B, Mark J. In-situ precipitation of reinforcing titania fillers. *Polym Bull*. 1987;17(3):271-7. doi: <https://doi.org/10.1007/BF00285360>.
- 369 5. McCarthy D, Mark J, Schaefer D. Synthesis, structure, and properties of hybrid organic–inorganic composites based on polysiloxanes. I. Poly
370 (dimethylsiloxane) elastomers containing silica. *J Polym Sci, Part B: Polym Phys*. 1998;36(7):1167-89. doi: [https://doi.org/10.1002/\(SICI\)1099-0488\(199805\)36:7%3C1167::AID-POLB7%3E3.0.CO;2-R](https://doi.org/10.1002/(SICI)1099-0488(199805)36:7%3C1167::AID-POLB7%3E3.0.CO;2-R).
- 371 6. Yuan QW, Mark JE. Reinforcement of poly (dimethylsiloxane) networks by blended and in-situgenerated silica fillers having various sizes, size
372 distributions, and modified surfaces. *Macromol Chem Phys*. 1999;200(1):206-20. doi: [https://doi.org/10.1002/\(SICI\)1521-3935\(19990101\)200:1%3C206::AID-MACP206%3E3.0.CO;2-S](https://doi.org/10.1002/(SICI)1521-3935(19990101)200:1%3C206::AID-MACP206%3E3.0.CO;2-S).
- 373 7. Hajji P, David L, Gerard J, Pascault J, Vigier G. Synthesis, structure, and morphology of polymer–silica hybrid nanocomposites based on
374 hydroxyethyl methacrylate. *J Polym Sci, Part B: Polym Phys*. 1999;37(22):3172-87. doi: [https://doi.org/10.1002/\(SICI\)1099-0488\(19991115\)37:22%3C3172::AID-POLB2%3E3.0.CO;2-R](https://doi.org/10.1002/(SICI)1099-0488(19991115)37:22%3C3172::AID-POLB2%3E3.0.CO;2-R).
- 375 8. Matějka L, Dukh O, Kolařík J. Reinforcement of crosslinked rubbery epoxies by in-situ formed silica. *Polymer*. 2000;41(4):1449-59. doi:
376 [https://doi.org/10.1016/S0032-3861\(99\)00317-1](https://doi.org/10.1016/S0032-3861(99)00317-1).
- 377 9. Matějka L, Dukh O. Organic-inorganic hybrid networks. *Macromolecular Symposia*: Wiley Online Library; 2001. p. 181-8.
- 378 10. Dewimille L, Bresson B, Bokobza L. Synthesis, structure and morphology of poly (dimethylsiloxane) networks filled with in situ generated
379 silica particles. *Polymer*. 2005;46(12):4135-43. doi: <https://dx.doi.org/10.1016/j.polymer.2005.02.049>.
- 380 11. Bokobza L, Diop A. Reinforcement of poly (dimethylsiloxane) by sol-gel in situ generated silica and titania particles. *Express Polymer Letters*.
381 2010;4(6):355-63. doi: <http://dx.doi.org/10.3144/expresspolymlett.2010.45>.
- 382 12. Wen J, Mark JE. Precipitation of silica-titania mixed-oxide fillers into poly (dimethylsiloxane) networks. *Rubber Chem Technol*.
383 1994;67(5):806-19. doi: <https://doi.org/10.5254/1.3538712>.
- 384 13. Breiner J, Mark J. Preparation, structure, growth mechanisms and properties of siloxane composites containing silica, titania or mixed silica–
385 titania phases. *Polymer*. 1998;39(22):5483-93. doi: [https://doi.org/10.1016/S0032-3861\(98\)02897%2910276-2](https://doi.org/10.1016/S0032-3861(98)02897%2910276-2).
- 386 14. Giannelis EP. Polymer layered silicate nanocomposites. *Adv Mater*. 1996;8(1):29-35. doi: <https://doi.org/10.1002/adma.19960080104>.
- 387 15. Krishnamoorti R, Vaia RA, Giannelis EP. Structure and dynamics of polymer-layered silicate nanocomposites. *Chem Mater*. 1996;8(8):1728-
388 34. doi: <https://doi.org/10.1021/cm960127g>.
- 389
- 390
- 391

392
393
394
395
396
397
398
399
400
401
402
403
404
405
406
407
408
409
410
411
412
413
414
415
416
417
418
419
420
421
422
423
424
425
426
427
428
429
430
431
432
433
434
435
436
437
438
439
440
441
442
443
444
445
446
447
448
449
450
451
452
453
454
455
456
457
458
459
460
461
462
463
464
465
466
467
468
469
470
471
472
473
474
475
476
477
478
479
480
481
482
483
484

16. Alexandre M, Dubois P. Polymer-layered silicate nanocomposites: preparation, properties and uses of a new class of materials. *Materials science and engineering: R: Reports*. 2000;28(1-2):1-63. doi: [https://doi.org/10.1016/S0927-796X\(00\)00012-7](https://doi.org/10.1016/S0927-796X(00)00012-7).
17. Okada A, Usuki A. Twenty years of polymer-clay nanocomposites. *Macromolecular materials and Engineering*. 2006;291(12):1449-76. doi: <https://doi.org/10.1002/mame.200600260>.
18. Bokobza L. Spectroscopic techniques for the characterization of polymer nanocomposites: A review. *Polymers*. 2018;10(1):7. doi: <https://doi.org/10.3390/polym10010007>.
19. Bokobza L, Rahmani M, Belin C, Bruneel JL, El Bounia NE. Blends of carbon blacks and multiwall carbon nanotubes as reinforcing fillers for hydrocarbon rubbers. *J Polym Sci, Part B: Polym Phys*. 2008;46(18):1939-51. doi: <https://doi.org/10.1002/polb.21529>.
20. Galimberti M, Coombs M, Cipolletti V, Riccio P, Riccò T, Pandini S, et al. Enhancement of mechanical reinforcement due to hybrid filler networking promoted by an organoclay in hydrocarbon-based nanocomposites. *Applied clay science*. 2012;65:57-66. doi: <https://doi.org/10.1016/j.clay.2012.04.019>.
21. Ma P-C, Siddiqui NA, Marom G, Kim J-K. Dispersion and functionalization of carbon nanotubes for polymer-based nanocomposites: a review. *Composites Part A: Applied Science and Manufacturing*. 2010;41(10):1345-67. doi: <https://doi.org/10.1016/j.compositesa.2010.07.003>.
22. Punetha VD, Rana S, Yoo HJ, Chaurasia A, McLeskey Jr JT, Ramasamy MS, et al. Functionalization of carbon nanomaterials for advanced polymer nanocomposites: A comparison study between CNT and graphene. *Prog Polym Sci*. 2017;67:1-47. doi: <https://doi.org/10.1016/j.progpolymsci.2016.12.010>.
23. Zhang X, Hou L, Samori P. Coupling carbon nanomaterials with photochromic molecules for the generation of optically responsive materials. *Nature communications*. 2016;7(1):1-14. doi: <https://doi.org/10.1038/ncomms11118>.
24. Singh V, Joung D, Zhai L, Das S, Khondaker SI, Seal S. Graphene based materials: past, present and future. *Prog Mater Sci*. 2011;56(8):1178-271. doi: <https://doi.org/10.1016/j.pmatsci.2011.03.003>.
25. Xu L, Cheng L. Graphite oxide under high pressure: a Raman spectroscopic study. *Journal of Nanomaterials*. 2013;2013. doi: <https://doi.org/10.1155/2013/731875>.
26. Kim HJ, Lee S-M, Oh Y-S, Yang Y-H, Lim YS, Yoon DH, et al. Unoxidized graphene/alumina nanocomposite: fracture-and wear-resistance effects of graphene on alumina matrix. *Sci Rep*. 2014;4(1):1-10. doi: <https://doi.org/10.1038/srep05176>.
27. Bokobza L, Bruneel J-L, Couzi M. Raman spectra of carbon-based materials (from graphite to carbon black) and of some silicone composites. *C—Journal of Carbon Research*. 2015;1(1):77-94. doi: <https://doi.org/10.3390/c1010077>.
28. Viculis LM, Mack JJ, Mayer OM, Hahn HT, Kaner RB. Intercalation and exfoliation routes to graphite nanoplatelets. *J Mater Chem*. 2005;15(9):974-8. doi: <https://doi.org/10.1039/B413029D>.
29. Geng Y, Wang SJ, Kim J-K. Preparation of graphite nanoplatelets and graphene sheets. *Journal of colloid and interface science*. 2009;336(2):592-8. doi: <https://doi.org/10.1016/j.jcis.2009.04.005>.
30. Kuilla T, Bhadra S, Yao D, Kim NH, Bose S, Lee JH. Recent advances in graphene based polymer composites. *Prog Polym Sci*. 2010;35(11):1350-75. doi: <https://doi.org/10.1016/j.progpolymsci.2010.07.005>.
31. Li B, Zhong W-H. Review on polymer/graphite nanoplatelet nanocomposites. *Journal of materials science*. 2011;46(17):5595-614. doi: <https://doi.org/10.1007/s10853-011-5572-y>.
32. Sengupta R, Bhattacharya M, Bandyopadhyay S, Bhowmick AK. A review on the mechanical and electrical properties of graphite and modified graphite reinforced polymer composites. *Prog Polym Sci*. 2011;36(5):638-70. doi: <https://doi.org/10.1016/j.progpolymsci.2010.11.003>.
33. Cai M, Thorpe D, Adamson DH, Schniepp HC. Methods of graphite exfoliation. *J Mater Chem*. 2012;22(48):24992-5002. doi: <https://doi.org/10.1039/C2JM34517J>.
34. Papageorgiou DG, Kinloch IA, Young RJ. Graphene/elastomer nanocomposites. *Carbon*. 2015;95:460-84. doi: <https://doi.org/10.1016/j.carbon.2015.08.055>.
35. Dimiev AM, Ceriotti G, Metzger A, Kim ND, Tour JM. Chemical mass production of graphene nanoplatelets in~ 100% yield. *ACS nano*. 2016;10(1):274-9. doi: <https://pubs.acs.org/doi/abs/10.1021/acsnano.5b06840>.
36. Schadler L, Brinson L, Sawyer W. Polymer nanocomposites: a small part of the story. *JOM*. 2007;59(3):53-60. doi: <https://doi.org/10.1007/s11837-007-0040-5>.
37. Park N-M, Kim T-S, Park S-J. Band gap engineering of amorphous silicon quantum dots for light-emitting diodes. *Appl Phys Lett*. 2001;78(17):2575-7. doi: <https://doi.org/10.1063/1.1367277>.
38. Bueche A. Filler reinforcement of silicone rubber. *Journal of Polymer Science*. 1957;25(109):139-49. doi: <https://doi.org/10.1002/pol.1957.1202510902>.
39. Barna E, Bommer B, Kürsteiner J, Vital A, Trzebiatowski Ov, Koch W, et al. Innovative, scratch proof nanocomposites for clear coatings. *Composites Part A: Applied Science and Manufacturing*. 2005;36(4):473-80. doi: <https://doi.org/10.1016/j.compositesa.2004.10.014>.
40. Wichmann MH, Sumfleth J, Gojny FH, Quaresimin M, Fiedler B, Schulte K. Glass-fibre-reinforced composites with enhanced mechanical and electrical properties—benefits and limitations of a nanoparticle modified matrix. *Engineering Fracture Mechanics*. 2006;73(16):2346-59. doi: <https://doi.org/10.1016/j.engfracmech.2006.05.015>.
41. Liu T, Phang IY, Shen L, Chow SY, Zhang W-D. Morphology and mechanical properties of multiwalled carbon nanotubes reinforced nylon-6 composites. *Macromolecules*. 2004;37(19):7214-22. doi: <https://doi.org/10.1021/ma049132t>.
42. Xia Z, Riestler L, Curtin W, Li H, Sheldon B, Liang J, et al. Direct observation of toughening mechanisms in carbon nanotube ceramic matrix composites. *Acta Mater*. 2004;52(4):931-44. doi: <https://doi.org/10.1016/j.actamat.2003.10.050>.
43. Ash BJ, Siegel RW, Schadler LS. Mechanical behavior of alumina/poly (methyl methacrylate) nanocomposites. *Macromolecules*. 2004;37(4):1358-69. doi: <https://doi.org/10.1021/ma0354400>.
44. Naous W, Yu XY, Zhang QX, Naito K, Kagawa Y. Morphology, tensile properties, and fracture toughness of epoxy/Al₂O₃ nanocomposites. *J Polym Sci, Part B: Polym Phys*. 2006;44(10):1466-73. doi: <https://doi.org/10.1002/polb.20800>.
45. Ma D, Siegel RW, Hong J-I, Schadler LS, Mårtensson E, Örneby C. Influence of nanoparticle surfaces on the electrical breakdown strength of nanoparticle-filled low-density polyethylene. *J Mater Res*. 2004;19(3):857-63. doi: <https://doi.org/10.1557/jmr.2004.19.3.857>.
46. Bokobza L. Investigation of local dynamics of polymer chains in the bulk by the excimer fluorescence technique. *Prog Polym Sci*. 1990;15(3):337-60. doi: [https://doi.org/10.1016/0079-6700\(90\)90001-H](https://doi.org/10.1016/0079-6700(90)90001-H).
47. George GA. Characterization of solid polymers by luminescence techniques. *Pure Appl Chem*. 1985;57(7):945-54. doi: <https://doi.org/10.1351/pac198557070945>.
48. Zammarano M, Maupin PH, Sung L-P, Gilman JW, McCarthy ED, Kim YS, et al. Revealing the interface in polymer nanocomposites. *ACS nano*. 2011;5(4):3391-9. doi: <https://doi.org/10.1021/nn102951n>.
49. Maupin PH, Gilman JW, Harris Jr RH, Bellayer S, Bur AJ, Roth SC, et al. Optical Probes for Monitoring Intercalation and Exfoliation in Melt-Processed Polymer Nanocomposites. *Macromol Rapid Commun*. 2004;25(7):788-92. doi: <https://doi.org/10.1002/marc.200300262>.
50. Rittigstein P, Torkelson JM. Polymer–nanoparticle interfacial interactions in polymer nanocomposites: confinement effects on glass transition temperature and suppression of physical aging. *J Polym Sci, Part B: Polym Phys*. 2006;44(20):2935-43. doi: <https://doi.org/10.1002/polb.20925>.
51. Clough JM, Creton C, Craig SL, Sijbesma RP. Covalent bond scission in the Mullins effect of a filled elastomer: real-time visualization with mechanoluminescence. *Adv Funct Mater*. 2016;26(48):9063-74. doi: <https://doi.org/10.1002/adfm.201602490>.
52. Böhme U, Scheler U. Interfaces in polymer nanocomposites—An NMR study. *AIP Conference Proceedings: AIP Publishing LLC*; 2016. p. 090009.
53. Bovey FA, Mirau PA. *NMR of Polymers*. Academic Press; 1996.
54. Schmidt-Rohr K, Spiess HW. Multidimensional solid-state NMR and polymers. Elsevier; 2012.
55. Mirau PA, Heffner SA, Schilling M. Fast magic-angle spinning proton NMR studies of polymers at surfaces and interfaces. *Solid State Nucl Magn Reson*. 2000;16(1-2):47-53. doi: [https://doi.org/10.1016/S0926-2040\(00\)00053-9](https://doi.org/10.1016/S0926-2040(00)00053-9).
56. Avolio R, Gentile G, Avella M, Capitani D, Errico ME. Synthesis and characterization of poly (methylmethacrylate)/silica nanocomposites: Study of the interphase by solid-state NMR and structure/properties relationships. *J Polym Sci, Part A: Polym Chem*. 2010;48(23):5618-29. doi: <https://doi.org/10.1002/pola.24377>.
57. Li W, Hou L, Chen Z. An NMR investigation of phase structure and chain dynamics in the polyethylene/montmorillonite nanocomposites. *Journal of Nanomaterials*. 2013;2013. doi: <https://doi.org/10.1155/2013/937210>.
58. Rodrigues T, Tavares MI, Soares I, Moreira A, Ferreira A. The use of solid state NMR to characterize high density polyethylene/organoclay nanocomposites. *Chemistry and chemical technology* 2009. doi: <http://ena.lp.edu.ua:8080/handle/ntb/7213>.
59. Cole KC. Use of infrared spectroscopy to characterize clay intercalation and exfoliation in polymer nanocomposites. *Macromolecules*. 2008;41(3):834-43. doi: <https://doi.org/10.1021/ma0628329>.
60. Zhang X, Bhuvana S, Loo LS. Characterization of layered silicate dispersion in polymer nanocomposites using Fourier transform infrared spectroscopy. *J Appl Polym Sci*. 2012;125(S1):E175-E80. doi: <https://doi.org/10.1002/app.36266>.

485
486
487
488
489
490
491
492
493
494
495
496
497
498
499
500
501
502
503
504
505
506
507
508
509
510
511
512
513
514
515
516
517
518
519
520
521
522
523
524
525
526
527
528
529
530
531
532
533
534
535
536
537
538
539
540
541
542
543
544
545
546
547
548
549
550
551
552
553
554
555
556
557
558
559
560
561
562
563
564
565
566
567
568

61. Titus E, Ali N, Cabral G, Gracio J, Babu PR, Jackson M. Chemically functionalized carbon nanotubes and their characterization using thermogravimetric analysis, Fourier transform infrared, and Raman spectroscopy. *J Mater Eng Perform*. 2006;15(2):182-6. doi: <https://doi.org/10.1361/105994906X95841>.

62. Hussain S, Jha P, Chouksey A, Raman R, Islam S, Islam T, et al. Spectroscopic investigation of modified single wall carbon nanotube (SWCNT). *Journal of Modern Physics*. 2011;2(06):538. doi: <http://dx.doi.org/10.4236/jmp.2011.26063>.

63. Ngo CL, Le QT, Ngo TT, Nguyen DN, Vu MT. Surface modification and functionalization of carbon nanotube with some organic compounds. *Advances in Natural Sciences: Nanoscience and Nanotechnology*. 2013;4(3):035017. doi: <https://doi.org/10.1088/2043-6262/4/3/035017>.

64. Lee SH, Choi SH, Kim SY, Choi JI, Lee JR, Youn JR. Degradation and dynamic properties of poly (amide-co-imide)/carbon nanotube composite films. *Polym Polym Compos*. 2010;18(7):381-90. doi: <https://doi.org/10.1177%2F096739111001800704>.

65. Deniz AE, Vural HA, Ortaç B, Uyar T. Gold nanoparticle/polymer nanofibrous composites by laser ablation and electrospinning. *Mater Lett*. 2011;65(19-20):2941-3. doi: <https://doi.org/10.1016/j.matlet.2011.06.045>.

66. Al-Attabi NY, Kaur G, Adhikari R, Cass P, Bown M, Evans M, et al. Preparation and characterization of highly conductive polyurethane composites containing graphene and gold nanoparticles. *Journal of Materials Science*. 2017;52(19):11774-84. doi: <https://doi.org/10.1007/s10853-017-1335-8>.

67. Kausar A. Polyaniline composites with nanodiamond, carbon nanotube and silver nanoparticle: Preparation and properties. *American Journal of Polymer Science & Engineering*. 2015;3(2):149-60. doi: <http://www.ivyunion.org/index.php/ajpse/>.

68. Bokobza L. Filled elastomers: A new approach based on measurements of chain orientation. *Polymer*. 2001;42(12):5415-23. doi: [https://doi.org/10.1016/S0032-3861\(00\)00853-3](https://doi.org/10.1016/S0032-3861(00)00853-3).

69. Bokobza L. Infrared analysis of elastomeric composites under uniaxial extension. *Macromolecular Symposia*: Wiley Online Library; 2005. p. 45-60.

70. Besbes S, Cermelli I, Bokobza L, Monnerie L, Bahar I, Erman B, et al. Segmental orientation in model networks of poly (dimethylsiloxane): Fourier-transform infrared dichroism measurements and theoretical interpretation. *Macromolecules*. 1992;25(7):1949-54. doi: <https://doi.org/10.1021/ma00033a018>.

71. Cole KC, Perrin-Sarazin F, Dorval-Douville G. Infrared Spectroscopic Characterization of Polymer and Clay Platelet Orientation in Blown Films Based on Polypropylene-Clay Nanocomposite. *Macromolecular symposia*: Wiley Online Library; 2005. p. 1-10.

72. Bokobza L, Garnaud G, Beaunier P, Bruneel J-L. Vibrational and electrical investigations of a uniaxially stretched polystyrene/carbon nanotube composite. *Vib Spectrosc*. 2013;67:6-13. doi: <https://doi.org/10.1016/j.vibspec.2013.03.002>.

73. Dazzi A, Prater CB. AFM-IR: Technology and applications in nanoscale infrared spectroscopy and chemical imaging. *Chem Rev*. 2017;117(7):5146-73. doi: <https://doi.org/10.1021/acs.chemrev.6b00448>.

74. Marcott C, Lo M, Dillon E, Kjoller K, Prater C. Interface analysis of composites using AFM-based nanoscale IR and mechanical spectroscopy. *Microscopy Today*. 2015;23(2):38-45. doi: <https://doi.org/10.1017/S1551929515000036>.

75. Iijima S. Helical microtubules of graphitic carbon. *nature*. 1991;354(6348):56-8. doi: <https://doi.org/10.1038/354056a0>.

76. Bokobza L, Couzi M, Bruneel J-L. Raman spectroscopy of polymer-carbon nanomaterial composites. *Rubber Chem Technol*. 2017;90(1):37-59. doi: https://doi.org/10.1533/9780857091390_2_400.

77. Bounos G, Andrikopoulos KS, Karachalios TK, Voyiatzis GA. Evaluation of multi-walled carbon nanotube concentrations in polymer nanocomposites by Raman spectroscopy. *Carbon*. 2014;76:301-9. doi: <https://doi.org/10.1016/j.carbon.2014.04.081>.

78. Everall N, Lumsdon J, Christopher D. The effect of laser-induced heating upon the vibrational Raman spectra of graphites and carbon fibres. *Carbon*. 1991;29(2):133-7. doi: [https://doi.org/10.1016/0008-6223\(91\)90064-P](https://doi.org/10.1016/0008-6223(91)90064-P).

79. Yan X, Kitahama Y, Sato H, Suzuki T, Han X, Itoh T, et al. Laser heating effect on Raman spectra of styrene-butadiene rubber/multiwalled carbon nanotube nanocomposites. *Chem Phys Lett*. 2012;523:87-91. doi: <https://doi.org/10.1016/j.cplett.2011.11.082>.

80. Kao C, Young R. A Raman spectroscopic investigation of heating effects and the deformation behaviour of epoxy/SWNT composites. *Compos Sci Technol*. 2004;64(15):2291-5. doi: <https://doi.org/10.1016/j.compscitech.2004.01.019>.

81. Bokobza L, Zhang J. Raman spectroscopic characterization of multiwall carbon nanotubes and of composites. *Express Polymer Letters*. 2012;6(7). doi: <http://dx.doi.org/10.3144/expresspolymlett.2012.63>.

82. Bokobza L, Bruneel J-L, Couzi M. Raman spectroscopic investigation of carbon-based materials and their composites. Comparison between carbon nanotubes and carbon black. *Chem Phys Lett*. 2013;590:153-9. doi: <https://doi.org/10.1016/j.cplett.2013.10.071>.

83. Srivastava I, Mehta RJ, Yu Z-Z, Schadler L, Koratkar N. Raman study of interfacial load transfer in graphene nanocomposites. *Appl Phys Lett*. 2011;98(6):063102. doi: <https://doi.org/10.1063/1.3552685>.

84. Beigbeder A, Linares M, Devalckenaere M, Degée P, Claes M, Beljonne D, et al. CH-n Interactions as the Driving Force for Silicone-Based Nanocomposites with Exceptional Properties. *Adv Mater*. 2008;20(5):1003-7. doi: <https://doi.org/10.1002/adma.200701497>.

85. Bokobza L. Some issues in rubber nanocomposites: New opportunities for silicone materials. *Silicon*. 2009;1(3):141-5. doi: <https://doi.org/10.1007/s12633-009-9010-6>.

86. Frogley MD, Ravich D, Wagner HD. Mechanical properties of carbon nanoparticle-reinforced elastomers. *Compos Sci Technol*. 2003;63(11):1647-54. doi: [https://doi.org/10.1016/S0266-3538\(03\)00066-6](https://doi.org/10.1016/S0266-3538(03)00066-6).

87. Kumar N, Mignuzzi S, Su W, Roy D. Tip-enhanced Raman spectroscopy: principles and applications. *EPJ Techniques and Instrumentation*. 2015;2(1):9. doi: <https://doi.org/10.1140/epjt/s40485-015-0019-5>.

88. Kuroski D. Advances of tip-enhanced Raman spectroscopy (TERS) in electrochemistry, biochemistry, and surface science. *Vib Spectrosc*. 2017;91:3-15. doi: <https://doi.org/10.1016/j.vibspec.2016.06.004>.

89. Saito Y, Yanagi K. Using a nano light source to investigate small-scale composite materials. *Citeseer*; 2008.

90. Yano T-a, Inouye Y, Kawata S. Nanoscale uniaxial pressure effect of a carbon nanotube bundle on tip-enhanced near-field Raman spectra. *Nano Lett*. 2006;6(6):1269-73. doi: <https://doi.org/10.1021/nl060108y>.

91. Yano T-a, Ichimura T, Kuwahara S, H'Dhili F, Uetsuki K, Okuno Y, et al. Tip-enhanced nano-Raman analytical imaging of locally induced strain distribution in carbon nanotubes. *Nature communications*. 2013;4(1):1-7. doi: <https://doi.org/10.1038/ncomms3592>.

92. Vantasin S, Yan X-I, Suzuki T, Ozaki Y. Tip-Enhanced Raman Scattering of Nanomaterials. *e-Journal of Surface Science and Nanotechnology*. 2015;13:329-38. doi: <https://doi.org/10.1380/ejssnt.2015.329>.

93. Suzuki T, Yan X, Kitahama Y, Sato H, Itoh T, Miura T, et al. Tip-enhanced Raman spectroscopy study of local interactions at the interface of styrene-butadiene rubber/multiwalled carbon nanotube nanocomposites. *The Journal of Physical Chemistry C*. 2013;117(3):1436-40. doi: <https://doi.org/10.1021/jp309217y>.

94. Giesfeldt KS, Connatser RM, De Jesús MA, Dutta P, Sepaniak MJ. Gold-polymer nanocomposites: studies of their optical properties and their potential as SERS substrates. *Journal of Raman Spectroscopy: An International Journal for Original Work in all Aspects of Raman Spectroscopy, Including Higher Order Processes, and also Brillouin and Rayleigh Scattering*. 2005;36(12):1134-42. doi: <https://doi.org/10.1002/jrs.1418>.

95. Fateixa S, Giro AV, Nogueira HI, Trindade T. Polymer based silver nanocomposites as versatile solid film and aqueous emulsion SERS substrates. *J Mater Chem*. 2011;21(39):15629-36. doi: <https://doi.org/10.1039/C1JM12444G>.

96. Rao VK, Radhakrishnan T. Tuning the SERS response with Ag-Au nanoparticle-embedded polymer thin film substrates. *ACS applied materials & interfaces*. 2015;7(23):12767-73. doi: <https://doi.org/10.1021/acsami.5b04180>.

97. Biswas A, Bayer IS, Dahanayaka DH, Bumm LA, Li Z, Watanabe F, et al. Tailored polymer-metal fractal nanocomposites: an approach to highly active surface enhanced Raman scattering substrates. *Nanotechnology*. 2009;20(32):325705. doi: <https://doi.org/10.1088/0957-4484/20/32/325705>.

98. Schlücker S. Surface-Enhanced Raman spectroscopy: Concepts and chemical applications. *Angew Chem Int Ed*. 2014;53(19):4756-95. doi: <https://doi.org/10.1002/anie.201205748>.

99. Chang J, Zhi X, Zhang A. Application of Graphene in Surface-Enhanced Raman Spectroscopy. *Nano Biomedicine & Engineering*. 2017;9(1). doi: <https://doi.org/10.5101/NBE.V9I1.P49-56>.

100. Carboni D, Lasio B, Alzari V, Mariani A, Loché D, Casula MF, et al. Graphene-mediated surface enhanced Raman scattering in silica mesoporous nanocomposite films. *Physical Chemistry Chemical Physics*. 2014;16(47):25809-18. doi: <https://doi.org/10.1039/C4CP03582H>.